Pergamon

Int. J. Heat Mass Transfer. Vol. 37, No. 13, pp. 1885–1897, 1994

0017-9310/94 $7.00 + 0.00

0017-9310(94)E0015-M

Enhancement of natural convection heat transfer of an enclosure by a rotating circular cylinder

WU-SHUNG FU, CHAO-SHENG CHENG and WEN-JIANN SHIEH

Department of Mechanical Engineering, National Chiao Tung University, 1001 Ta Hsueh Road, Hsinchu 30050 Taiwan, Republic of China

(*Received* 11 *November* 1992 *and in final form* 13 *December* 1993)

Abstract—Enhancement of natural convection heat transfer in an enclosure by a rotating cylinder is investigated numerically. A penalty finite-element method with a Newton–Raphson iteration algorithm is adopted to solve the governing equations with the boundary conditions, and the accuracy of solutions is sensitively affected by the grid system combining curve-sided and rectangular quadrilateral elements. Since the flow fields of fluids are induced by mutual interaction between the natural convection and the rotating cylinder, the contribution of the rotating cylinder to natural convection heat transfer depends on the direction of rotation of the cylinder. For the counter-clockwise rotating cylinder situation, the contribution is found to be substantial when the value of Gr/Re^2 is larger than 100; however, for the clockwise rotation cylinder situation, the contribution is hardly found even when the value of Gr/Re^2 is equal to 1.

INTRODUCTION

THE STUDY of natural convection in an enclosure has been investigated for decades due to its extensive applications in engineering, like solar energy systems, electronic cooling equipment, crystal growth processes, etc. At an early stage, the study was mostly focused on the steady-state problem, and Ostrach [1] and Catton [2] had reviewed it in detail. Afterward, Nansteel and Grief [3], Lin and Bejan [4], Bajorek and Lloyd [5], Zimmerman and Acharya [6], Jetli *et al.* [7], and Fu and Shieh [8] investigated natural convection in a partially divided enclosure. In general, the natural convection decays in this kind of problem. However, in many practical engineering applications, the convection flow of most influence in an enclosure may consist mainly of the transient or unsteady-state type. Thus Nicolette *et al.* [9], Patterson and Imberger [10], Chorin [11], Yewell *et al.* [12], Ivey [13], Khalilollahi and Sammakia [14], and Fu *et al.* [15, 16] investigated natural convection in an enclosure at transient state to examine the variation processes of flow and thermal fields. Besides, Fu and Shieh [17] studied natural convection in an enclosure under the time-dependent gravitational acceleration field to simulate the enclosure set in a flying vehicle. Furthermore, Gershuni and Zhukhoritsk [18], Forbes *et al.* [19], Biringen and Danabasoglu [20], and Fu and Shieh [21] investigated thermal convection in an enclosure induced simultaneously by gravity and vibration, and found that the variations of thermal and flow fields are very complicated and the heat transfer of natural convection is usually increased. Based upon the literature mentioned above, the enclosure subjected to vibration condition seems to be the only method to enhance the natural convection in an enclosure. However, not only the numerical and experimental studies for the natural convection in an enclosure under vibration condition are extraordinarily complex, but also the device used in engineering applications is difficult to perform. Therefore, a method of employing a rotating circular cylinder which will strengthen the flow induced by thermal difference in an enclosure shown in Fig. 1 is proposed to enhance the minute natural convection heat transfer of the enclosure.

In accordance with this objective, this study employs a numerical method to investigate the enhancement of natural convection of a square enclosure in which a rotation circular cylinder is set. Due to the calculation boundary composed of the square

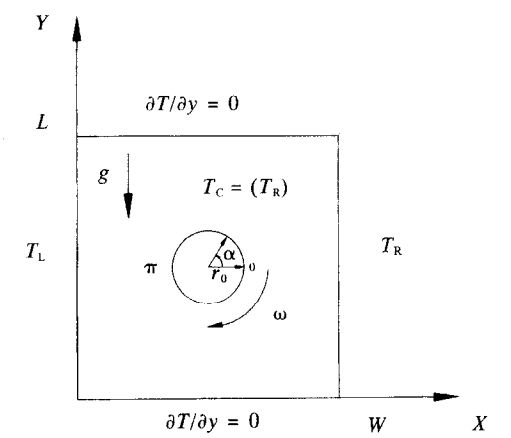

FIG. 1. Physical model.

NOMENCLATURE

Ar	ratio of L to $2r_0$ ($= L/2r_0$)
C	circular cylinder
c_p	specific heat [J kg^{-1} K^{-1}]
$CCWR$	counter-clockwise rotating
CWR	clockwise rotating
Gr	Grashof number ($= g\beta(T_L - T_R)L^3/\nu^2$)
g	gravitational acceleration [m s^{-2}]
h	natural convection coefficient [W m^{-2} K^{-1}]
k	thermal conductivity [W m K^{-1}]
L	height of enclosure [m]
Nu	local Nusselt number ($= hL/k$)
Nu_T	total Nusselt number
P^*	pressure [Pa]
P_d	motion pressure ($= P^* + \rho_c gy$) [Pa]
Pr	Prandtl number ($= c_p \cdot \mu/k$)
Re	Reynolds number ($= u_{max} 2r_0/\nu$)
r_0	radius of circular cylinder [m]
T	temperature [K]
u_{max}	velocity ($r_0\omega$) [m s^{-1}]
u, v	velocities in x and y directions [m s^{-1}]
U, V	dimensionless velocities in x and y directions
W	width of enclosure [m]
x, y	coordinates.

Greek symbols

α	angle of circular cylinder [rad]
β	thermal expansion coefficient [1/K]
θ	dimensionless temperature ($= (T - T_R)/(T_L - T_R)$)
μ	viscosity [Pa s]
ν	kinematic viscosity [m^2 s^{-1}]
ρ	density [kg m^{-3}]
ω	rotating speed [rad s^{-1}].

Subscripts

C	cylinder
L	left wall
R	right wall
T	total.

enclosure and circular cylinder, the numerical method of finite element, which is flexible and effective for an irregular calculation boundary, is adopted to solve the governing equations. Meanwhile, an out-of-core skyline method is utilized to reduce massive computer memory. The Grashof numbers of 10^4, 10^5, and 10^6, and clockwise and counter-clockwise rotating directions of the cylinder are taken into consideration. The important index of Gr/Re^2 varies from 10^5 to 10^0 for Grashof numbers of 10^4 and 10^5, and from 10^5 to 10^1 for Grashof number of 10^6. The results show that when the rotating direction of the cylinder is counter-clockwise the natural convection is enhanced from the value of Gr/Re^2 being 10^3, while the natural convection is hardly enhanced under the clockwise rotating direction situation. In addition, the local Nusselt number distributions along the walls and velocity vector diagram are also illustrated.

PHYSICAL MODEL

The proposed physical model for this study is sketched in Fig. 1. A rotating circular cylinder with radius r_0 is set in an enclosure, which is two-dimensional with width W and height L ($W = L$); both the upper and lower walls of the enclosure are adiabatic. The left and right walls are, respectively, maintained at high temperature T_L and low temperature T_R. The temperature and rotating speed of the cylinder are T_C and ω, respectively. T_C is equal to T_R. Therefore, the flow of fluid in the enclosure is affected by both the temperature difference of the left and right walls, and in turn natural convection, and the rotating cylinder simultaneously.

To facilitate the analyses, the following assumptions are made:

(1) the fluid is Newtonian, and the flow is laminar; (2) the Boussinesq approximation is valid; and (3) radiation effect is neglected.

With these assumptions and the introduction of the dimensionless variables:

$$X = \frac{x}{L} \quad Y = \frac{y}{L} \quad Ar = \frac{L}{2r_0}$$

$$U = \frac{u}{u_{max}} \quad V = \frac{v}{u_{max}} \quad P = \frac{p_d}{\rho u_{max}^2}$$

$$Re = \frac{u_{max} 2r_0}{\nu} \quad \theta = \frac{T - T_R}{T_L - T_R}$$

$$Pr = \frac{c_p \mu}{k} \quad Gr = \frac{g\beta(T_L - T_R)L^3}{\nu^2}, \tag{1}$$

where

$$P_d = P^* + \rho_R gy, \quad u_{max} = r_0\omega,$$

the dimensionless governing equations can be expressed as:

$$\frac{\partial U}{\partial X} + \frac{\partial V}{\partial Y} = 0, \tag{2a}$$

$$U\frac{\partial U}{\partial X} + V\frac{\partial U}{\partial Y} = -\frac{\partial P}{\partial X} + \frac{1}{Re}\left(\frac{\partial^2 U}{\partial X^2} + \frac{\partial^2 U}{\partial Y^2}\right)\frac{1}{Ar}, \tag{2b}$$

$$U\frac{\partial V}{\partial X}+V\frac{\partial V}{\partial Y}=-\frac{\partial P}{\partial Y}+\frac{1}{Re}\left(\frac{\partial^2 V}{\partial X^2}+\frac{\partial^2 V}{\partial Y^2}\right)\frac{1}{Ar}+\frac{Gr\,\theta}{Re^2}\frac{1}{Ar^2}, \quad (2c)$$

$$U\frac{\partial \theta}{\partial X}+V\frac{\partial \theta}{\partial Y}=\frac{1}{Pr\,Re}\left(\frac{\partial^2 \theta}{\partial X^2}+\frac{\partial^2 \theta}{\partial Y^2}\right)\frac{1}{Ar}. \quad (2d)$$

The boundary conditions are as follows:

$$X=0,\quad U=V=0,\quad \theta=1,$$

$$X=1,\quad U=V=0,\quad \theta=0,$$

$$Y=0,\quad U=V=0,\quad \frac{\partial \theta}{\partial Y}=0,$$

$$Y=1,\quad U=V=0,\quad \frac{\partial \theta}{\partial Y}=0.$$

On the cylinder surface:

$$\theta=0,$$

$$U=\pm\sin\alpha,$$

$$V=\pm\cos\alpha.$$

The sign "+" or "−" depends on the rotating direction of the cylinder.

SOLUTION METHOD

In essence, a penalty finite element method with a modified Newton–Raphson algorithm similar to the one used in Fu *et al.* [21] is employed to solve the governing equations (2a)–(2d). The detail of the numerical method is delineated in ref. [21]. Due to a circular cylinder set in a square enclosure, the grid system, which is different from that used in ref. [21], employed in this study is shown in Fig. 2, r_1 is the maximum distance of the array of curved-sided quadrilateral elements, and the array of curved-sided quadrilateral elements is denser than that of rectangular quadrilateral elements. Except the convergence criterion:

$$\left|\frac{\varphi^{m+1}-\varphi^{m}}{\varphi^{m+1}}\right|<10^{-3},\quad \varphi=U,V\text{ and }\theta,$$

used in [21], the following criterion which is lower than 1% is added:

$$E(\%)=\frac{Nu_{\mathrm{L}},T-(Nu_{\mathrm{C}},T+Nu_{\mathrm{R}},T)}{Nu_{\mathrm{L}},T}\times 100\%, \quad (3)$$

in which

$$Nu_{\varphi},T=\int_0^1 Nu_{\varphi}\,\mathrm{d}Y\ (\varphi=\mathrm{L}\text{ and }\mathrm{R}),$$

Nu_{φ}: local Nusselt number on the left or right wall,

$$Nu_{\mathrm{C}},T=\int_0^{2\pi r_0/L} Nu_{\mathrm{C}}\,\mathrm{d}S,$$

Nu_{C}: local Nusselt number on the cylinder surface, and $\mathrm{d}S$: dimensionless infinitesimal distance along the circular cylinder.

To validate the accuracy of the numerical method, the results of numerical tests are separately shown in the following figures. When the position of the cylinder is set at $(0.5L, 0.5L)$ and the direction of rotating is counter-clockwise, the $E(\%)$s under different Grashof numbers and grid systems are shown in Fig. 3. The lower the Grashof number, the larger the $E(\%)$ becomes. The $E(\%)$s of all situations are under 1%. Shown in Fig. 4 is the effect of (r_1/r_0) on the $E(\%)$: when the value of (r_1/r_0) is larger than 7, the $E(\%)$ is smaller than 1%. At this situation, the elements in the circumferential direction are 16 and in the radial direction are 7. Consequently, the array used of rectangular quadrilateral elements and curved-sided quadrilateral elements are 20×20 and 16×7, respectively. The ratio of r_1 to r_0 is 7. In all situations, the residual divergence of continuity equation of the summation of every grid is smaller than 10^{-3}.

RESULTS AND DISCUSSION

The fluid in the enclosure is air and the Prandtl number is 0.7. The ratio of r_0 to L is equal to 0.01. For examining the effect of rotation speed of the cylinder on the natural convection heat transfer of the enclosure, the values of 100, 10, and 1 of Gr/Re^2, and 10^4, 10^5, and 10^6 of Grashof numbers are mainly taken into consideration. Concerning the rotating direction of the cylinder, both clockwise and counter-clockwise directions are considered.

The cylinder is set at $(0.1L, 0.5L)$ and $(0.5L, 0.5L)$, respectively. However, the stratified layer is formed in the center region [15] and the center point is far away from the hot wall: thus the effect of the rotating cylinder set in the center region on the natural convection of the enclosure is slight. Owing to the limitation of space, the results of the cylinder set at $(0.1L, 0.5L)$ are represented exclusively.

Shown in Fig. 5 are velocity vectors, illustrated in the enclosure. Since the elements are arranged densely near the cylinder and the velocity vectors near the cylinder are much larger than those of another region, then the velocity vectors near the cylinder are not indicated to avoid interfering with other velocity vectors. In Fig. 5a, the velocities of fluids which flow orderly from the upper to lower region near the right wall zone are not affected by the rotating cylinder, which is set close to the left wall. In comparison, the velocities of fluids near the left wall region vary drastically due to the existence of the rotating cylinder. In Fig. 5b, the velocity vectors near the left wall are locally enlarged in order to more clearly examine the variations of velocity vectors. The sign of the arrow for the value of U defined by $u/u_{\max}$ shown above the figure is the maximum vector illustrated in the figure. Since the natural convection effect is strong under $Gr/Re^2=100$ situation, then the velocities of fluids

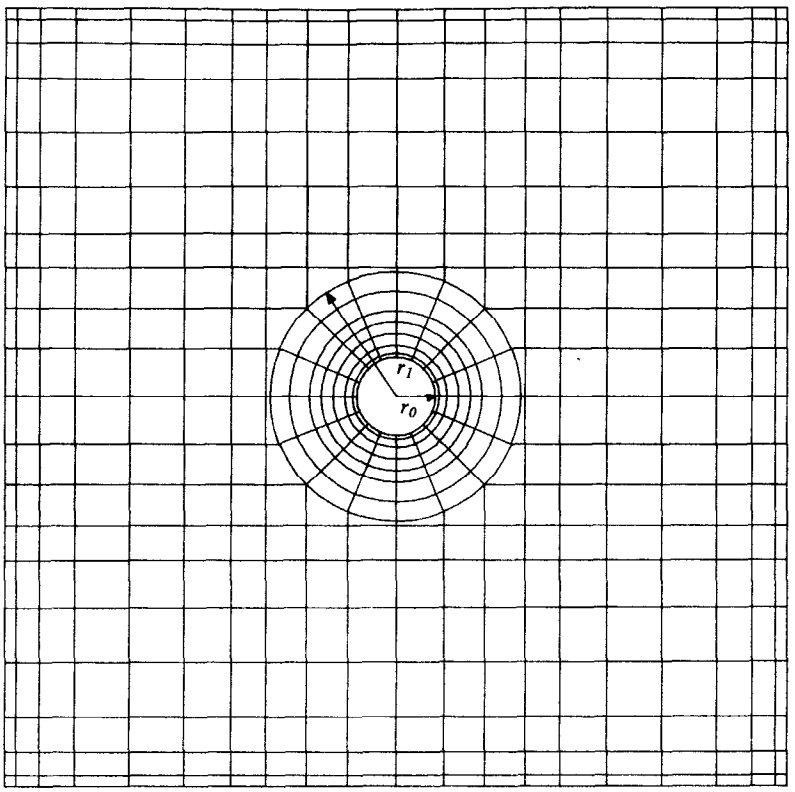

FIG. 2. Computational grid system.

which flow upward along the left wall are not affected by the rotating cylinder until $Y \cong 0.4$. Owing to the clockwise rotating cylinder, the flow directions of fluid induced by both the natural convection and rotating cylinder are consistent in the region between the left wall and the cylinder at $Y = 0.5$. Consequently, below $Y = 0.5$ the velocities of fluids near the left wall are accelerated gradually which enhances the heat transfer rate of the left wall, whereas the velocities of fluids in the region near (0.2, 0.4) are distorted by the rotating cylinder and turn to upper right direction. Due to the domination of the natural convection, over $Y = 0.6$ the fluids turn back to left wall and flow upward along the left wall.

The velocity vectors illustrated in Fig. 6 are for the $Gr/Re^2 = 1$ situation. The effect of the rotating

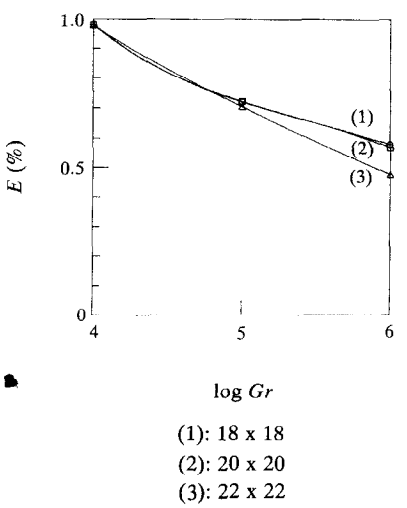

FIG. 3. Error test for grid systems [$r_0/L = 0.01$, $Gr/Re^2 = 10$, clockwise rotating cylinder].

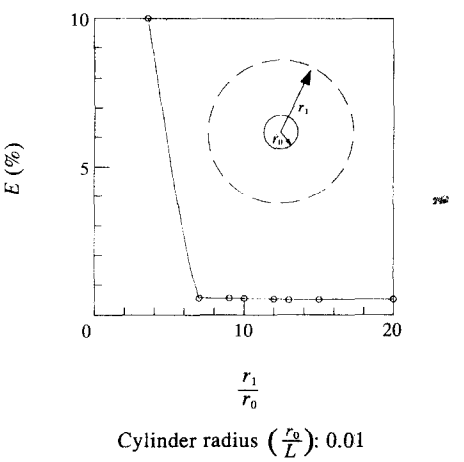

FIG. 4. Error test for the rations of (r_1/r_0) [$Gr = 10^6$, $Gr/Re^2 = 10$, clockwise rotating cylinder].

cylinder on the velocity of fluid is more remarkable than that of the former one because of the smaller value of Gr/Re^2. The velocities of fluids near the cylinder are solely affected by the cylinder which causes some fluids to impinge on the left wall at $Y \cong 0.42$ and rebound to the lower region. As a result, the fluids which flow from the bottom of the left wall turn to the upper right direction in advance, and are no longer accelerated as in the former situation. Due to the domination of the rotating cylinder, over $Y = 0.6$ part of the fluids on the right side of the cylinder are dragged and the directions of fluid velocities change to the lower left which causes a circulation zone to be formed. Even over $Y = 0.8$ the fluids are hardly observed to change direction to the left wall and flow upward continuously. Two circulation zones are formed on the upper and lower regions of the cylinder.

Shown in Figs. 7 and 8 the rotation direction of the cylinder is counter-clockwise and opposite to the former situation. In Fig. 7a, velocity vectors are distributed in the whole enclosure. The flow field near the left wall region is strongly affected by the rotating cylinder: the variation of the flow field is then drastic.

As shown in Fig. 7b, due to the counter-clockwise rotating cylinder, the fluids which flow upward from the bottom of the left wall induced by natural convection are easily accelerated, and flow upward from the right side of the cylinder. Above the cylinder, most of the fluids flow unanimously to the upper region of the left wall, but a few fluids flow downward along the left wall from $Y = 0.55$ to 0.45.

The velocity vectors shown in Fig. 8 are for the $Gr/Re^2 = 1$ situation. Since the directions of the fluid flow induced by both the natural convection and rotating cylinder are consistent in most regions, then the variation of flow field is comparatively monotonous. Consequently, the velocity vectors distributions for this situation are similar to those of the former one. The circulation zone can not be found out when the direction of the rotating cylinder is counter-clockwise.

The isothermal lines distributions for both the clockwise rotating (CWR) and counter-clockwise rotating ($CCWR$) cylinders are illustrated in Fig. 9. Near the rotating cylinder, the isothermal lines form concentric circles. The circulation zones mentioned earlier are formed on the upper and lower sides of the clockwise rotating cylinder which causes the isothermal lines to be distorted intensively. On the other hand, the directions of flow induced by the natural convection and counter-clockwise rotating cylinder in most of the regions are consistent, which results in the relatively simple variations of isothermal lines distributions.

The local Nusselt numbers distributed on the left wall (curve A), right wall (curve B), and rotating

C.W.R.

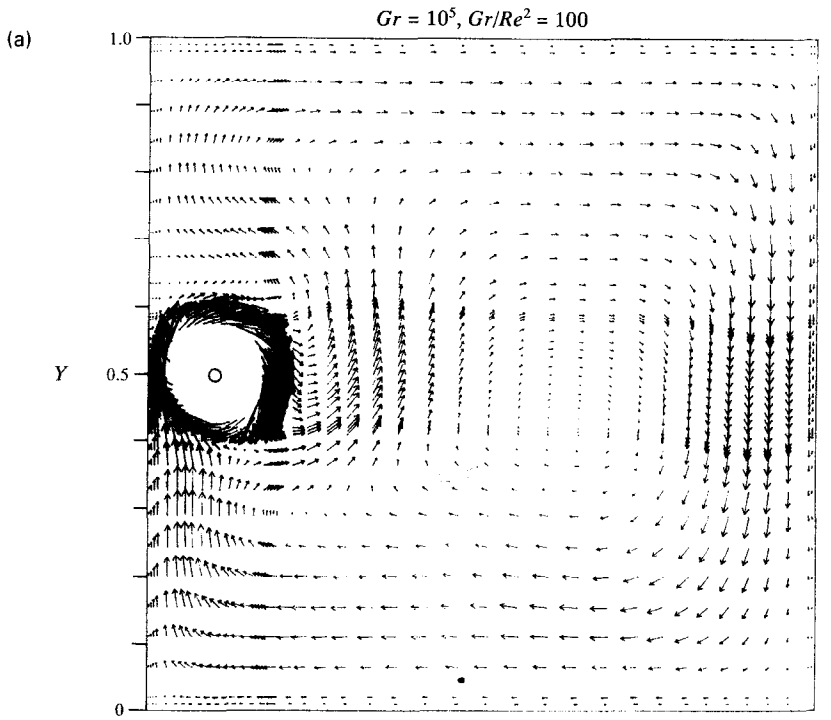

FIG. 5. (a) Velocity vectors distribution in the enclosure for $Gr = 10^5$, $Gr/Re^2 = 100$, clockwise rotating cylinder. (b) Velocity vectors distribution near the left wall for $Gr = 10^5$, $Gr/Re^2 = 100$, clockwise rotating cylinder.

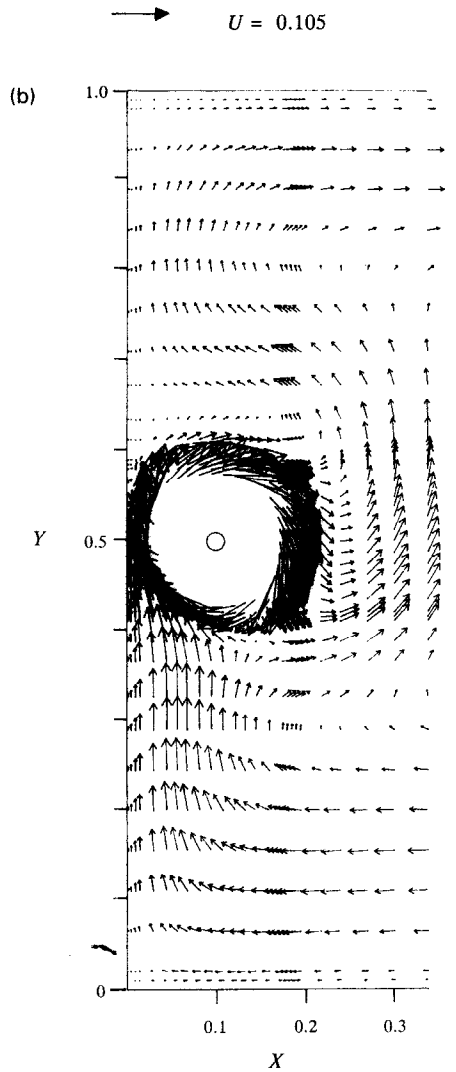

FIG. 5—*continued.*

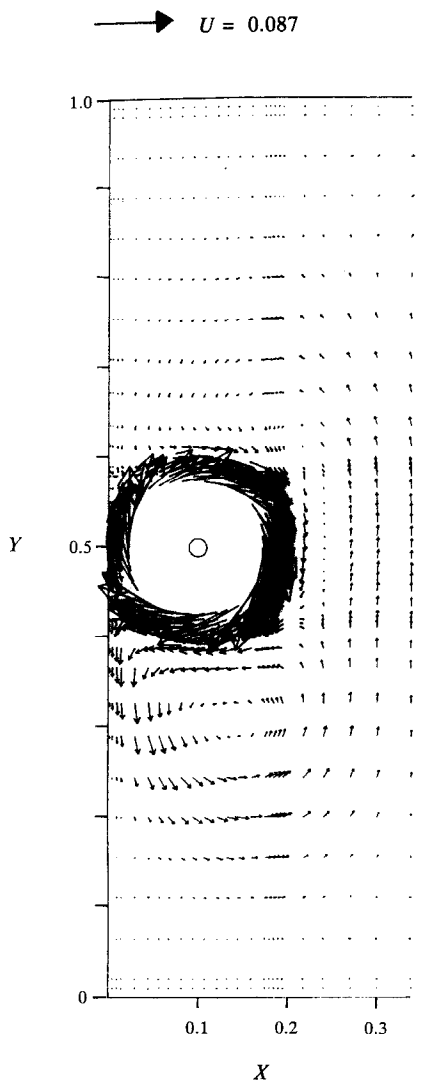

FIG. 6. Velocity vectors distribution near the left wall for $Gr = 10^5$, $Gr/Re^2 = 1$, clockwise rotating cylinder.

cylinder are illustrated in Figs. 10 and 11. Because the cylinder not only is set close to the center of the left wall but also is rotating, the local Nusselt numbers distributed near the center of the left wall are usually larger than those of another region. For $Gr/Re^2 = 100$ situation shown in Fig. 10a, the natural convection effect is remarkable, Fig. 5b; then the local Nusselt numbers in the region, in addition to the center region, of the lower left wall are relatively larger than those on the upper left wall region. The phenomenon is also observed for the $Gr/Re^2 = 10$ situation, shown in Fig. 10b. However for the $Gr/Re^2 = 1$ situation, the rotating speed of the cylinder becomes fast, and the velocities of fluids induced by natural convection are suppressed by the rotating cylinder shown in Fig. 6, which results in the smaller local Nusselt numbers distribution in the lower left wall region. Due to the domination of the rotating cylinder, the local Nusselt numbers distributed near the center region of the left wall become larger.

Concerning the local Nusselt numbers distribution on the right wall (curve B), the cylinder is set far away from the right wall and the effect of the cylinder on the local Nusselt numbers of the right wall is minute. Consequently, the variation of the local Nusselt numbers on the right wall is similar to that of the enclosure without the rotating cylinder.

As for the local Nusselt numbers Nu_c distribution on the cylinder shown in Fig. 10, the size of the cylinder is small and the rotating speed is relatively fast which causes the local Nusselt numbers distributed on the cylinder not to be affected by the left wall. As a result, the local Nusselt numbers are independent of the position of the cylinder and approximately constant. In essence, the smaller the value of Gr/Re^2 is, the larger the local Nusselt number becomes.

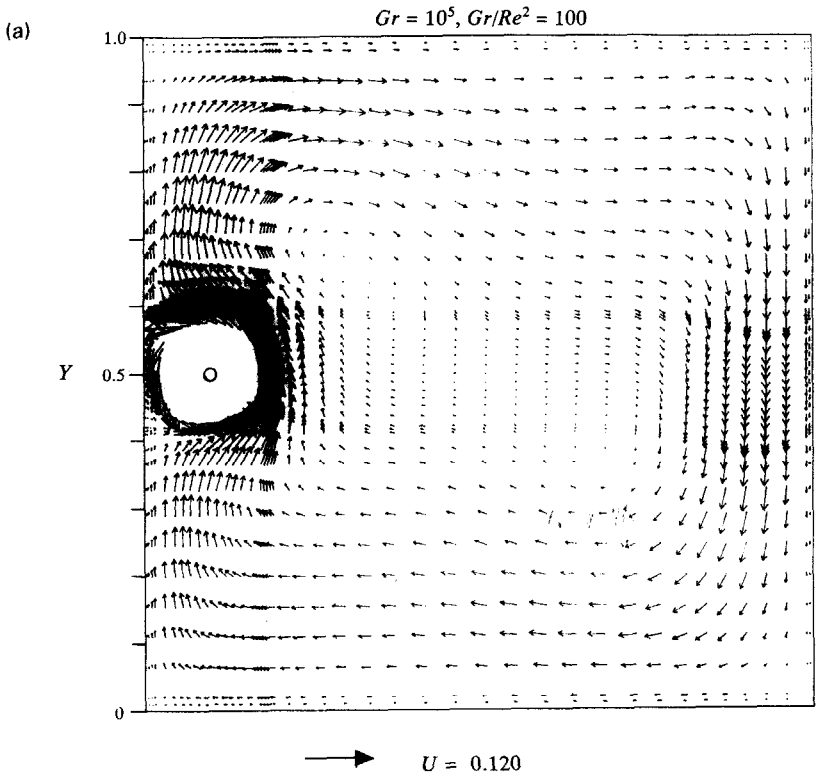

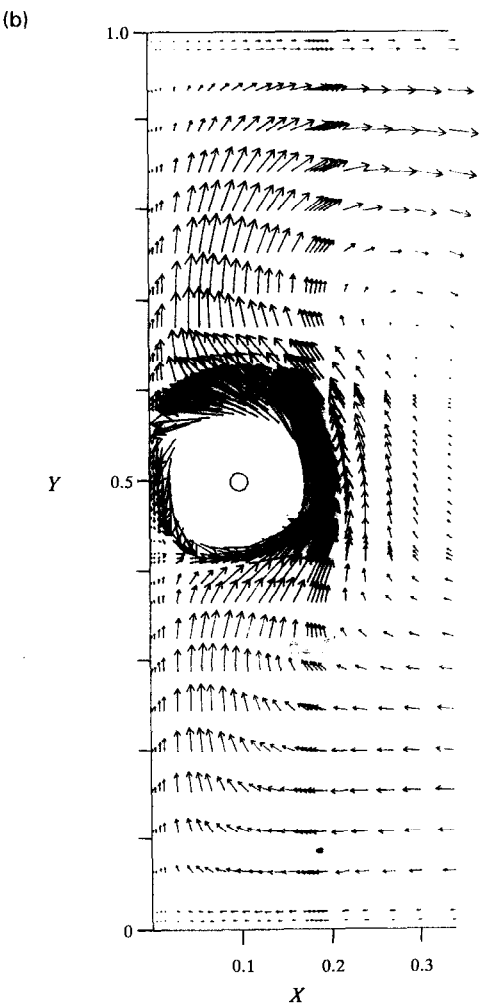

FIG. 7. (a) Velocity vectors distribution in the enclosure for $Gr = 10^5$, $Gr/Re^2 = 100$, counter-clockwise rotating cylinder. (b) Velocity vectors distribution near the left wall for $Gr = 10^5$, $Gr/Re^2 = 100$, counter-clockwise rotating cylinder.

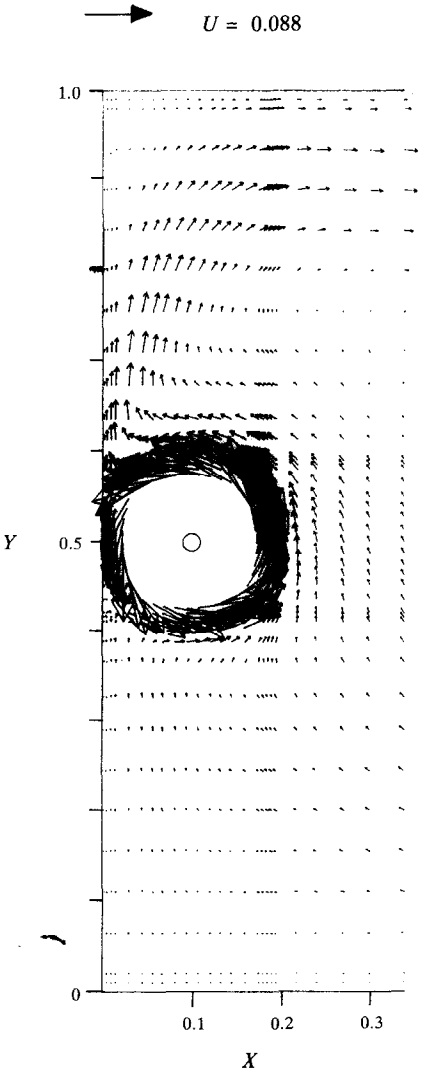

FIG. 8. Velocity vectors distribution near the left wall for $Gr = 10^5$, $Gr/Re^2 = 1$, counter-clockwise rotating cylinder.

Shown in Fig. 11, the local Nusselt numbers distributions are under the counter-clockwise rotating cylinder situation. In spite of the directions of the rotating cylinder, the effect of the rotating cylinder on the flow field of fluids near the cylinder is completely dominant. Consequently, the maximum local Nusselt number of the left wall usually occurs in the center region, and both the tendency of the variations and values of the local Nusselt numbers distributed on the cylinder are alike for the clockwise and counter-clockwise rotating cylinder situations. The velocities of fluids induced by the natural convection and counter-clockwise rotating cylinder are more consistent than those induced by the natural convection and clockwise rotating cylinder mentioned earlier which causes the local Nusselt numbers distributed on the left wall to be larger than those of the corresponding clockwise rotating cylinder situations indicated in former ones. But the tendency of variations of local Nusselt numbers on the left wall is similar for both the clockwise and counter-clockwise rotating cylinder situations. So do the local Nusselt numbers on the right wall.

As for the local Nusselt numbers on the cylinder, due to the consistency of the velocities of fluids induced by the natural convection and counter-clockwise rotating cylinder, the fluids impinge on the cylinder in a lower region initially: the slightly larger local Nusselt numbers then occur in the lower region of the cylinder shown in Fig. 11a. While the value of Gr/Re^2 decreases, the local Nusselt numbers tend to be constant.

In Fig. 12, total Nusselt numbers of the left wall (curve A), right wall (curve B), and cylinder (interval C) are indicated under different situations. As mentioned above the effects of the natural convection and clockwise rotating cylinder on the flow of fluids are easily mutually offset: therefore, except for $Gr = 10^4$ and $Gr/Re^2 = 1$, the clockwise rotating cylinder (CWR) hardly contributes to the total Nusselt number of the left wall in the calculation range. Under some situations, the total Nusselt numbers of the left wall even decrease. The reason suggested is that the fluids are impeded from flowing to the left wall due to the interaction of the natural convection and clockwise rotating cylinder near the left wall which is disadvantageous to the total Nusselt number of the left wall. The larger the Grashof number and the smaller the value of Gr/Re^2, the more remarkable this phenomenon is.

As for the counter-clockwise rotating cylinder ($CCWR$) situations, the effects of the natural convection and rotating cylinder on the flow of fluids are consistent with those mentioned earlier, which causes the counter-clockwise rotating cylinder to contribute to the Nusselt numbers of the left wall. As the value of Gr/Re^2 is about 10^3, the contribution of the rotating cylinder to the Nusselt number of the left wall begins to be revealed. The maximum enhancement of the Nusselt number of the left wall is about 60% for $Gr = 10^4$ and $Gr/Re^2 = 1$.

CONCLUSION

A penalty finite-element numerical method is used to investigate enhancement of natural convection of an enclosure by a rotating circular cylinder. Several conclusions can be drawn:

(1) The direction of the rotating cylinder plays a role in enhancing natural convection in an enclosure. In this study, the counter-clockwise rotating cylinder apparently contributes to the heat transfer rate, but the clockwise rotating cylinder does not.

(2) When the value of Gr/Re^2 is about 10^3, the enhancement of the heat transfer rate begins to be revealed. The maximum enhancement of the heat transfer rate is approximately equal to 60%.

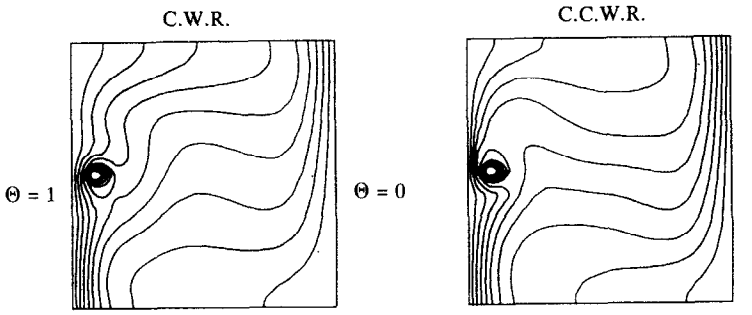

(a) $Gr/Re^2 = 100$

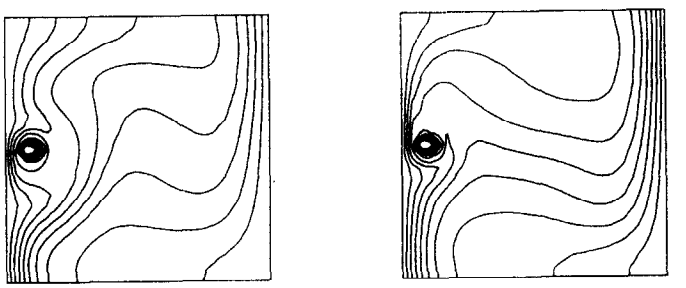

(b) $Gr/Re^2 = 10$

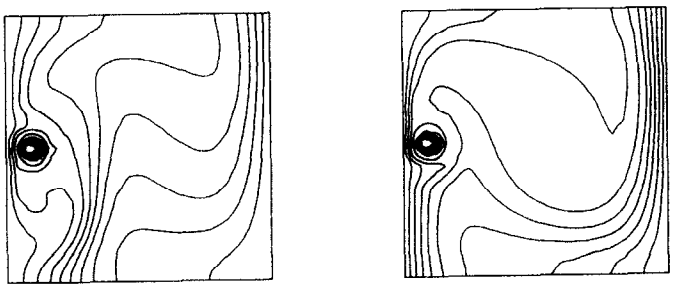

(c) $Gr/Re^2 = 1$

FIG. 9. Isothermal lines distributions for $Gr = 10^5$.

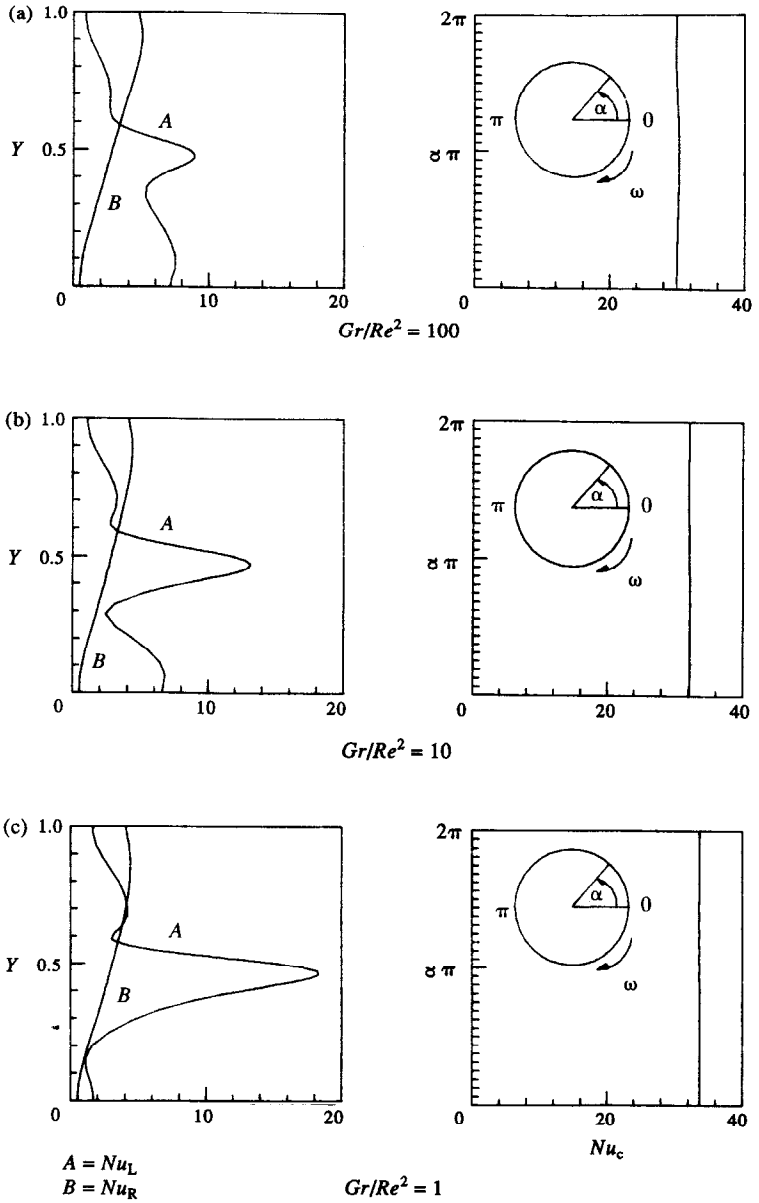

FIG. 10. Local Nusselt numbers distributions on the left, right, and cylinder walls for $Gr = 10^5$, clockwise rotating cylinder.

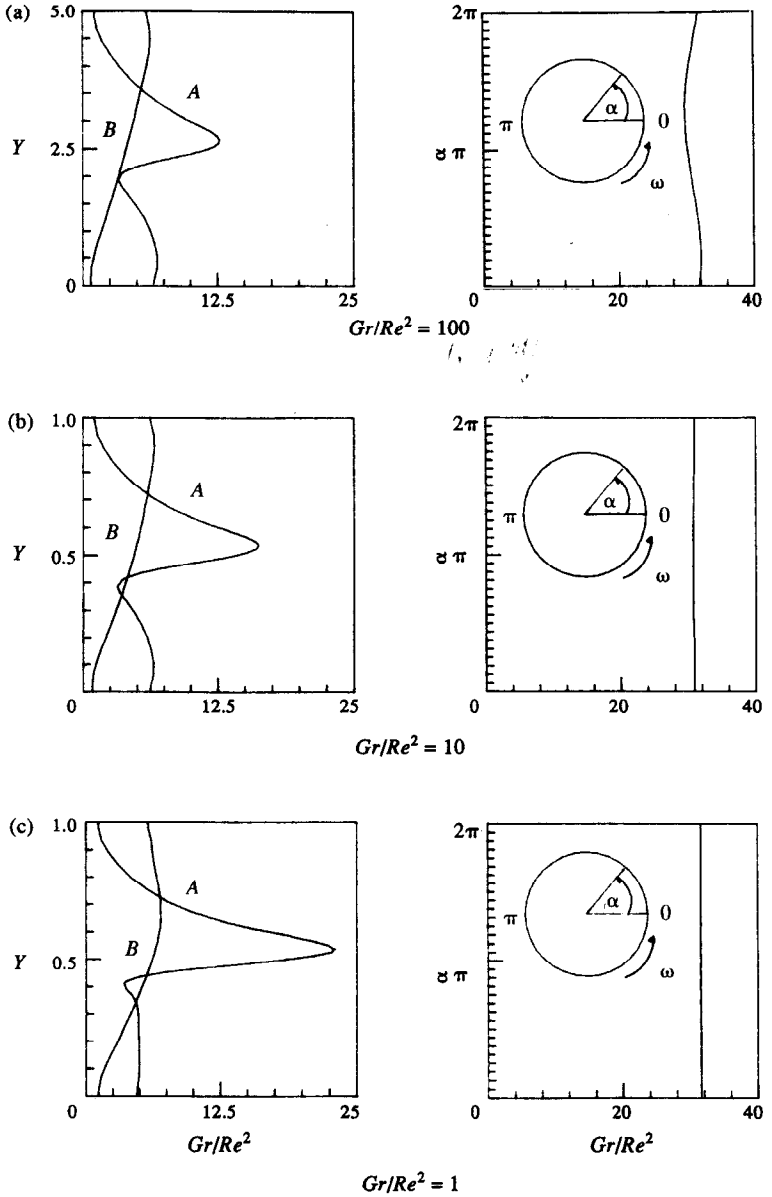

FIG. 11. Local Nusselt numbers distributions on the left, right, and cylinder walls for $Gr = 10^5$, counter-clockwise rotating cylinder.

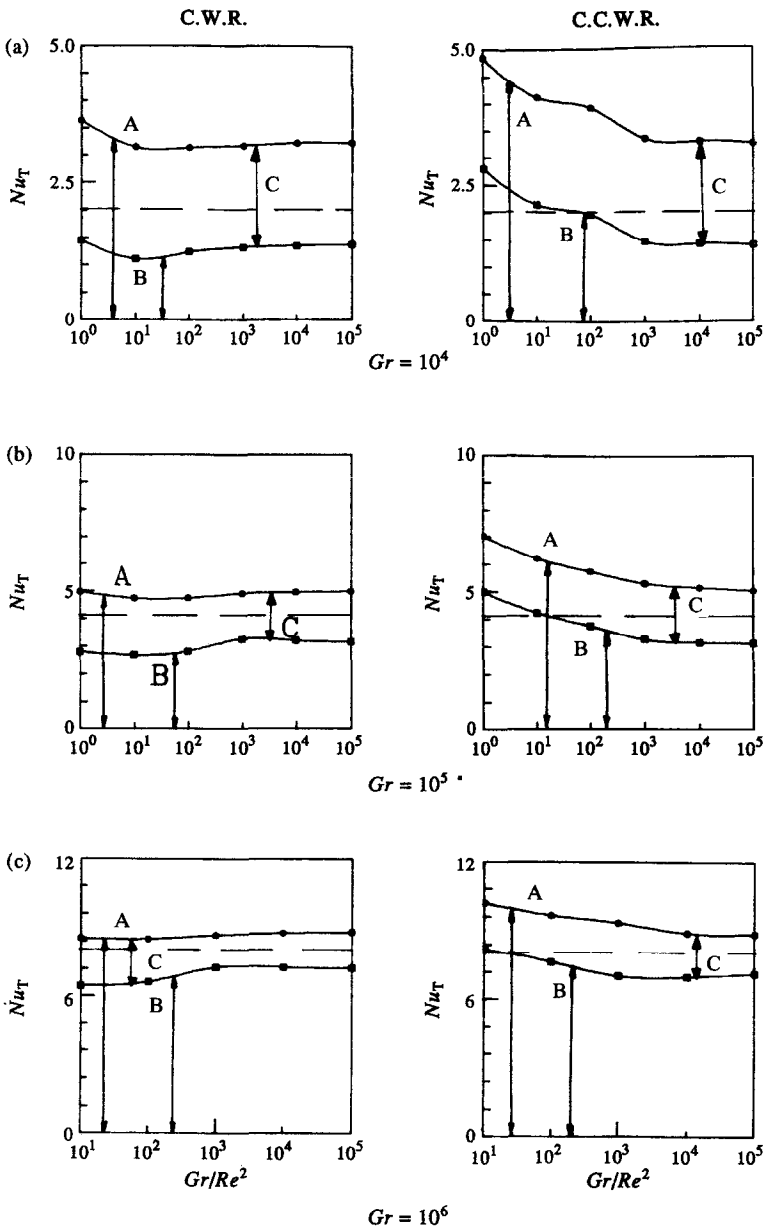

FIG. 12. Total Nusselt numbers on the left (A), right (B), and cylinder (C) walls.

Acknowledgement—The support of this work by the National Science Council, Taiwan, R.O.C. under the contract NSC81-0401-E009-530 is gratefully acknowledged.

REFERENCES

1. S. Ostrach, Natural convection in an enclosure, *Adv. Heat Transfer* 161–227 (1972).
2. I. Catton, Natural convection in an enclosure, *J. Heat Transfer* **6,** 13–43 (1978).
3. M. W. Nansteel and R. Grief, Natural convection in undivided and partially divided rectangular enclosures, *J. Heat Transfer* **103,** 623–629 (1981).
4. N. N. Lin and A. Bejan, Natural convection in a partially divided enclosure, *Int. J. Heat Mass Transfer* **26,** 1867–1878 (1983).
5. S. M. Bajorek and J. R. Lloyd, Experimental investigation of natural convection in partitioned enclosures, *J. Heat Transfer* **104,** 527–532 (1982).
6. E. Zimmerman and S. Acharya, Free convection heat transfer in a partially divided vertical enclosure with conducting end walls, *Int. J. Heat Mass Transfer* **30,** 319–332 (1987).
7. R. Jetli, S. Acharya and E. Zimmerman, Influence of baffle location on natural convection in a partially divided enclosure, *Numer. Heat Transfer* **10,** 521–536 (1986).
8. W. S. Fu and W. J. Shieh, A penalty finite element method for natural convection heat transfer in a partially divided enclosure, *Int. Comm. Heat Mass Transfer* **15,** 323–332 (1988).
9. V. F. Nicolette, K. T. Yang, and J. R. Lloyd, Transient cooling by natural convection in a two-dimensional square enclosure, *Int. J. Heat Mass Transfer* **28,** 1721–1731 (1985).

10. J. Patterson and J. Imberger, Unsteady natural convection in a rectangular cavity, *J. Fluid Mech.* **100,** 65–86 (1980).
11. A. J. Chorin, Numerical solution of the Navier–Stokes equations, *Math. Comput.* **22,** 745–762 (1968).
12. R. Yewell, D. Poulikakos and A. Bejan, Transient natural convection experiments in shallow enclosures, *J. Heat Transfer* **104,** 533–538 (1982).
13. G. N. Ivey, Experiments on transient natural convection in a cavity, *J. Fluid Meth.* **144,** 389–401 (1984).
14. A. Khalilollahi and B. Sammakia, Unsteady natural convection by a heated surface within an enclosure, *Numer. Heat Transfer* **9,** 715–730 (1986).
15. W. S. Fu, J. C. Perng, and W. J. Shieh, Transient laminar natural convection in an enclosure partitioned by an adiabatic baffle, *Numer. Heat Transfer* **16,** 325–350 (1989).
16. W. S. Fu, T. M. Kau and W. J. Shieh, Transient laminar natural convection in an enclosure from steady flow state to stationary state, *Numer. Heat Transfer* **18,** 189–212 (1990).
17. W. S. Fu and W. J. Shieh, A numerical study of transient natural convection under timer-dependent gravitational acceleration field, *Wärme und Stoffübertragung* **27,** 109–117 (1992).
18. G. Z. Gershuni and E. M. Zhukhovitsky, Vibrational thermal convection in zero gravity, *Fluid Mechanics—Soviet Research* **15,** 63–84 (1986).
19. R. E. Forbes, C. T. Carley and C. J. Bell, Vibration effects on convective heat transfer in enclosures, *J. Heat Transfer* **92,** 429–438 (1970).
20. S. Biringen and G. Danabasoglu, Computation of convective flow with gravity modulation in rectangular cavities, *J. Thermophysics* **4,** 357–365 (1990).
21. W. S. Fu and W. J. Shieh, A study of thermal convection in an enclosure induced simultaneously by gravity and vibration, *Int. J. Heat Mass Transfer* **35,** 1695–1710 (1992).